Hybrid Organic−Inorganic Membrane: Solving the Tradeoff between Permeability and Selectivity

Fubing Peng, Lianyu Lu, Honglei Sun, Yanqiang Wang, Jiaqi Liu, and Zhongyi Jiang*

Key Laboratory for Green Chemical Technology, Ministry of Education of China, School of Chemical Engineering and Technology, Tianjin University, Tianjin 300072, P. R. China

Received August 22, 2005. Revised Manuscript Received October 18, 2005

To solve the tradeoff between permeability and selectivity of polymeric membranes, organic−inorganic hybrid membranes composed of poly(vinyl alcohol) (PVA) and γ-glycidyloxypropyltrimethoxysilane (GPTMS) were prepared by an in situ sol−gel approach for pervaporative separation of benzene/cyclohexane mixtures. The structure of PVA-GPTMS hybrid membranes was characterized with FTIR, ^{29}Si NMR, SEM, TEM, and XRD. Energy-dispersive X-ray Si-mapping analysis demonstrated homogeneous dispersion of silica in the PVA matrix. Compared with pure PVA membranes, the hybrid membranes exhibited high thermal stability and lower T_g, and in particular improved pervaporation properties. Permeation flux increased from 20.3 g/(m^2 h) for pure PVA membrane to 137.1 g/(m^2 h) for PVA-GPTMS hybrid membrane with 28 wt % GPTMS content, and separation factor increased from 9.6 to 46.9 correspondingly. The pervaporation results of PVA-GPTMS hybrid membranes are all above the upper bound tradeoff curve (Lue, S. J.; Peng, S. H. *J. Membr. Sci.* **2003**, *222*, 203), while that of pure PVA membrane is obviously below the curve. Positron annihilation lifetime spectroscopy (PALS) was employed to elucidate the enhancement of permeation flux in polymer-based pervaporation membranes, and a size-selective mechanism was proposed to explain the enhancement of the separation factor.

Introduction

Membranes with both high permeability and selectivity are desirable for practical separation. Despite concentrated efforts to innovate polymer type and tailor polymer structure to improve separation properties, current polymeric membrane materials commonly suffer from the inherent drawback of tradeoff effect between permeability and selectivity,[1−3] which means that membranes more permeable are generally less selective and vice versa. On the other hand, although some inorganic membrane materials have shown rather good separation properties above the upper-bound tradeoff curve, which was constructed on an empirical basis for many gas or liquid pairs using published permeability and selectivity data, their large-scale application is still seriously restricted due to the poor processability and high capital cost. Therefore, it can be naturally envisaged that elaboration of hybrid membrane materials by bridging organic and inorganic components will be a convenient and efficient approach to cross the tradeoff hurdle.[4]

Organic−inorganic hybrid materials are promising systems for many applications due to their extraordinary properties arising from the synergism between the properties of these two different building blocks. A general classification to organic−inorganic hybrid materials has been proposed,[5−7] distinguishing "class I" materials, in which the inorganic and organic components interact through weak hydrogen bonding, van der Waals contacts, or electrostatic forces, from "class II" materials, in which the inorganic and organic components are linked through strong ionic/covalent bonding.

Organic−inorganic hybrid membranes have attracted considerable attention as potential "next generation" membrane materials.[8−10] Many researchers continue to explore the "class I" organic−inorganic membranes which are prepared by simply incorporating inorganic particles, such as zeolite,[11,12] carbon molecular sieve,[13] and silica,[9,14,15] into dense polymeric membranes to improve molecular separation properties. Merkel et al.[9,15] prepared poly(4-methyl-2-pentyne) (PMP) membranes containing nanoscale, nonporous fumed silica and found that contrary to behavior in traditional filled polymer systems, addition of fumed silica to glassy, amorphous PMP increases penetrant permeability by as much as 240%. They attributed the increase to increased free volume through disruption of polymer chain packing by inorganic filler. In a previous study, we[16] prepared crystalline

* To whom correspondence should be addressed. Tel.: +86-22-27892143. Fax: +86-22-27892143. E-mail: zhyjiang@tju.edu.cn.

(1) Freeman, B. D. *Macromolecules* **1999**, *32*, 375−380.
(2) Robeson, L. M. *J. Membr. Sci.* **1991**, *62*, 165.
(3) Lue, S. J.; Peng, S. H. *J. Membr. Sci.* **2003**, *222*, 203.
(4) Walcarius, A. *Chem. Mater.* **2001**, *13*, 3351−3372.
(5) Sanchez, C.; Ribot, F. *New J. Chem.* **1994**, *18*, 1007.
(6) Wen, J.; Wilkes, G. L. *Chem. Mater.* **1996**, *8*, 1667.
(7) Eckert, H.; Ward, M. *Chem. Mater.* **2001**, *13*, 3059−3060.
(8) Guizard, C.; Bac, A.; Barboiu, M.; Hovnanian, N. *Sep. Purif. Technol.* **2001**, *25*, 167.
(9) Merkel, T. C.; Freeman, B. D.; Spontak, R. J.; He, Z.; Pinnau, I.; Meakin, P.; Hill, A. J. *Science* **2002**, *296*, 519−522.
(10) Uragami, T.; Okazaki, K.; Matsugi, H.; Miyata, T. *Macromolecules* **2002**, *35*, 9156.
(11) te Hennepe, H. J. C.; Bargeman, D.; Mulder, M. H. V.; Smolders, C. A. *J. Membr. Sci.* **1987**, *35*, 39.
(12) Wang, H.; Holmberg, B. A.; Yan, Y. *J. Mater. Chem.* **2002**, *12*, 3640−3643.
(13) Peng, F. B.; Jiang, Z. Y.; Hu, C. L.; Wang, Y. Q.; Xu, H. Q.; Liu, J. Q. *Sep. Purif. Technol.* In press.
(14) Merkel, T. C.; He, Z.; Pinnau, I. *Macromolecules* **2003**, *36*, 6844.
(15) Merkel, T. C.; Freeman, B. D.; Spontak, R. J.; He, Z.; Pinnau, I.; Meakin, P.; Hill, A. J. *Chem. Mater.* **2003**, *15*, 109.

10.1021/cm051890q CCC: $30.25
Published on Web 11/24/2005

graphite flake filled poly(vinyl alcohol) membrane which introduced graphite to interfere with polymer chain packing and augmented free volume and, thus, obtained higher permeability. However, most filled polymeric membranes failed to cross the upper-bound tradeoff curve due to the following main disadvantages: agglomeration of inorganic particles and formation of nonselective voids, which usually exist at the interface of these two phases[17,18] since the interaction between inorganic particles and polymer is of physical origin. In a recent paper, Moore and Koros[19] have summarized the relationship between organic−inorganic membrane morphologies and transport properties and pointed out the tradeoff phenomenon mainly derived from the nonideal effects such as varying degrees of rigidification in the surrounding polymer, undesirable voids at the interfaces, and partial or total clogging of the dispersed phase. Therefore, we can imagine that "class II" hybrid organic−inorganic membranes will be a better solution.

The dominant processing method of the "class II" organic−inorganic membranes, which can efficiently avoid formation of nonselective void at the organic−inorganic interface and the agglomeration of inorganic particles, is based on the convenient and mild sol−gel process.[6,8,19−21] Kusakabe et al.[22] prepared polyurethane (PU) membranes containing tetraethyl orthosilicate (PU/TEOS) and applied them to benzene/cyclohexane fractionation. They found that benzene/cyclohexane selectivity in the hybrid membrane was higher than that in the PU counterpart. However, the permeation flux was lower in the hybrid membrane. Uragami et al.[10] and Kariduraganavar et al.[23,24] prepared PVA/TEOS hybrid membranes for pervaporation separation, which also showed decreased permeability and increased selectivity. Liu et al.[25] prepared organic−inorganic hybrid membranes composed of chitosan and GPTMS which exhibited decreased permeability and enhanced selectivity and thermal and chemical resistance.

Based on the solution-diffusion theory and free-volume theory, we believe that as long as we can prepare the organic−inorganic hybrid membranes with larger free volume and suitable size of the free volume cavity, the permeability and selectivity will be enhanced simultaneously. However, the successful preparation relies heavily on the appropriate recipe of the organic−inorganic hybrid membranes.

Among the commonly used hydrophilic polymers, PVA has found increasing applications as a pervaporation membrane material due to its superior properties. Furthermore, to improve the compatibility, mechanical properties of the hybrid membrane, appropriate selection of precursor with sufficient hydrophilicity and ideal structure is also crucial.[26−30] GPTMS, as a modified sol−gel precursor, seems an ideal candidate.[31,32] The opening of epoxy ring in GPTMS allows the formation of hydroxyl group, rendering the inorganic sols with higher hydrophilicity, and thus better compatibility with hydrophilic PVA. The hydroxyl groups in PVA molecule could form hydrogen bonds or become involved in the condensation reaction with silanols produced during hydrolysis of the precursor.[33]

In this study, novel PVA-GPTMS hybrid membranes with reversal tradeoff effect, i.e., simultaneously increased permeability and selectivity, were prepared. The structure, morphology, thermal stability, and dynamic mechanical properties of PVA-GPTMS hybrid membranes were investigated. To explain the enhancement of permeation flux and separation factor, free volume[34] characteristics of PVA-GPTMS hybrid membranes were investigated by PALS, which can be used to study the structure of PVA-GPTMS hybrid membrane at the molecular level and detect molecular vacancies of size equivalent to those of benzene or cyclohexane in the polymer-based pervaporation membranes.

Experimental Section

Materials. Poly(vinyl alcohol) (PVA) (Tianjin Yuanli Chemical Co. Ltd., degree of polymerization 1750±50) and γ-glycidyloxypropyltrimethoxysilane (GPTMS) (Nanjing Crompton Shuguang Organosilicon Specialties Group Co., Ltd.) were used as supplied. Benzene and cyclohexane (Tianjin Jiangtian Chemicals Ltd.) were of analytical grade and were used without further purification. Double-distilled water was used throughout the study.

Preparation of PVA-GPTMS Hybrid Membranes. PVA was dissolved in double-distilled water at 90 °C for 2 h to make 5 wt % PVA homogeneous solutions. A measured amount of GPTMS and 1.0 M HCl were then added at room temperature, and the mixture was stirred for 12 h. The PVA solutions with GPTMS loading of 0, 10, 17, 28, 37, and 45 wt % (the ratio of GPTMS weight to weight of PVA plus GPTMS) were cast on an organic glass plate, initially dried at room temperature overnight, and then dried at 120 °C for 2 h to obtain the final PVA-GPTMS hybrid membranes. The membranes were about 80 μm thick, measured with a micrometer. The resulting hybrid membranes are designated as PVA-GPTMS-X, where X indicates the weight percentage of GPTMS in the membranes.

Membrane Characterization. FTIR spectra were recorded on a Nicolet, 5DX instrument equipped with both horizontal attenuated

(16) Peng, F. B.; Lu, L. Y.; Hu, C. L.; Wu, H.; Jiang, Z. Y. *J. Membr. Sci.* **2005**, *259*, 65.
(17) Moore, T. T.; Mahajan, R.; Vu, D. Q.; Koros, W. J. *AIChE J.* **2004**, *50*, 311.
(18) Moore, T. T.; Koros, W. J. *J. Mol. Struct.* **2005**, *739*, 87−98.
(19) Nagarale, R. K.; Gohil, G. S.; Shahi, V. K.; Rangarajan, R. *Macromolecules* **2004**, *37*, 10025.
(20) Bronstein, L. M.; Joo, C.; Karlinsey, R.; Ryder, A.; Zwanziger, J. W. *Chem. Mater.* **2001**, *13*, 3678−3684.
(21) Gao, Y.; Choudhury, N. R.; Dutta, N.; Matisons, J.; Reading, M.; Delmotte, L. *Chem. Mater.* **2001**, *13*, 3644−3652.
(22) Kusakabe, K.; Yoneshige, S.; Morooka, S. *J. Membr. Sci.* **1998**, *149*, 29−37.
(23) Kariduraganavar, M. Y.; Kulkarni, S. S.; Kittur, A. A. *J. Membr. Sci.* **2005**, *246*, 83.
(24) Kulkarni, S. S.; Kittur, A. A.; Aralaguppi, M. I.; Kariduraganavar, M. Y. *J. Appl. Polym. Sci.* **2004**, *94*, 1304.
(25) Liu, Y.-L.; Su, Y.-H.; Lee, K.-R.; Lai, J.-Y. *J. Membr. Sci.* **2005**, *251*, 233.
(26) Uragami, T.; Katayama, T.; Miyata, T.; Tamura, H.; Shiraiwa, T.; Higuchi, A. *Biomacromolecules* **2004**, *5*, 1567.
(27) Park, S.-B.; You, J.-O.; Park, H.-Y.; Haam, S. J.; Kim, W.-S. *Biomaterials* **2001**, *22*, 323.
(28) Hsiue, G.-H.; Chen, J.-K.; Liu, Y.-L. *J. Appl. Polym. Sci.* **2000**, *76*, 1609.
(29) Cerveau, G.; Chappellet, S.; Corriu, R. J. P. *J. Mater. Chem.* **2003**, *13*, 2885.
(30) Wang, Q.; Liu, N.; Wang, X.; Li, J.; Zhao, X.; Wang, F. *Macromolecules* **2003**, *56*, 5760.
(31) Sarkhel, D.; Roy, D.; Bandyopadhyay, M.; Bhattacharya, P. *Sep. Purif. Technol.* **2003**, *30*, 89.
(32) Pandey, L. K.; Saxena, C.; Dubey, V. *J. Membr. Sci.* **2003**, *227*, 173.
(33) Shchipunov, Y. A.; Karpenko, T. Y. *Langmuir* **2004**, *20*, 3882.
(34) Budd, P. M.; McKeown, N. B.; Fritsch, D. *J. Mater. Chem.* **2005**, *15*, 1977.

total reflectance (HATR) accessories. Thirty-two scans were accumulated with a resolution of 4 cm^{-1} for each spectrum. Solid-state NMR spectra were recorded on an Infinity Plus-300 MHz spectrometer. Solid samples were spun at 3 kHz. Element mapping was conducted with a Philips XL30ESEM scanning electronic microscope equipped with energy-dispersive X-ray spectroscopy (EDX) of ISIS300 (Oxford). The microstructure of the hybrid membranes was examined by transmission electron microscopy (TEM) using a Tecnai G2 F20 instrument. Morphology of the PVA and hybrid membranes was studied using a Rigaku D/max 2500v/pc X-ray diffractometer in the range of 5−45° at the speed of 8°/min (Cu Kα 40 kV/200 mA). Thermogravimetric analysis (TGA) was conducted with a Perkin-Elmer TG/DTA thermogravimetric analyzer at a heating rate of 10 °C/min under a nitrogen atmosphere. Dynamic mechanical data were obtained with a Perkin-Elmer DMA instrument. All samples were tested within the temperature range of 298−500 K at a heating rate of 5 K/min, and a frequency of 1 Hz was selected for all the experiments.

Free Volume Analysis. PALS experiments were performed by using an EG&G ORTEC fast-fast coincidence system at room temperature. The PALS method is based on the so-called free volume model, which assumes that positronium (Ps) localizes in the free volume elements of the polymer structure because of its repulsion (exchange interaction) from the surrounding molecules.[35,36] Positronium can be formed in two states: para-positronium (p-Ps) is formed by two particles with opposite spin and ortho-positronium (o-Ps) is formed if the spins of the particles are parallel. In a vacuum p-Ps and o-Ps annihilate intrinsically with mean lifetimes of 0.125 and 142 ns, respectively. In polymers, annihilation with an electron localizing then occurs on the inner wall of the free volume cavity (pick-off process), reducing the lifetime of o-Ps (τ_{o-Ps}, i.e., τ_3 and τ_4) to 1−5 ns. A semiempirical equation given by eq 1 correlates τ_{o-Ps} with the radius of the free volume cavity, r. This is obtained by assuming that the o-Ps is localized in a spherical potential well surrounded by an electron layer of thickness Δr equal to 0.1656 nm.[37,38]

$$\tau = \frac{1}{2}\left[1 - \frac{r}{r+\Delta r} + \left(\frac{1}{2\pi}\right)\sin\left(\frac{2\pi r}{r+\Delta r}\right)\right]^{-1} \quad (1)$$

The intensity I gives the probability of o-Ps formation, and it is proportional to the number of free volume cavities in the system.

Pervaporation Experiment. The pervaporation properties of the hybrid membranes were investigated with benzene and cyclohexane mixture. Pervaporation experiments were performed on the P-28 membrane module (CM-Celfa AG Company, Switzerland). The effective surface area of the membrane in contact with feed is 28.0 cm^2. The vacuum in the downstream side was maintained (1 kPa) using a vacuum pump, and permeate was collected in liquid nitrogen cold traps. The compositions of the feed and permeate were measured using Agilent 6820 gas chromatography equipped with a FID detector and a PEG20M column. The pervaporation properties of the organic−inorganic hybrid membranes are evaluated by two parameters, flux J, which is defined as $J = W/At$, and separation factor α, which is defined as $\alpha = (y_B/y_C)/(x_B/x_C)$, where W is the mass of permeate collected in time t, A is the membrane area, and x and y represent the weight fractions of benzene (B) and cyclohexane (C) in the feed and permeate, respectively.

(35) Shrader, D. M., Jean, Y. C., Eds. *Positron and positronium chemistry*; Elsevier: Amsterdam, 1988.
(36) Hristov, H. A.; Bolan, B.; Yee, A. F.; Xie, L.; Gidley, D. W. *Macromolecules* **1996**, *29*, 8507.
(37) Tao, S. J. *J. Chem. Phys.* **1972**, *56*, 5499.
(38) Sharma, S. C. *Positronium annihilation studies of fluids*; World Science: Singapore, 1988.

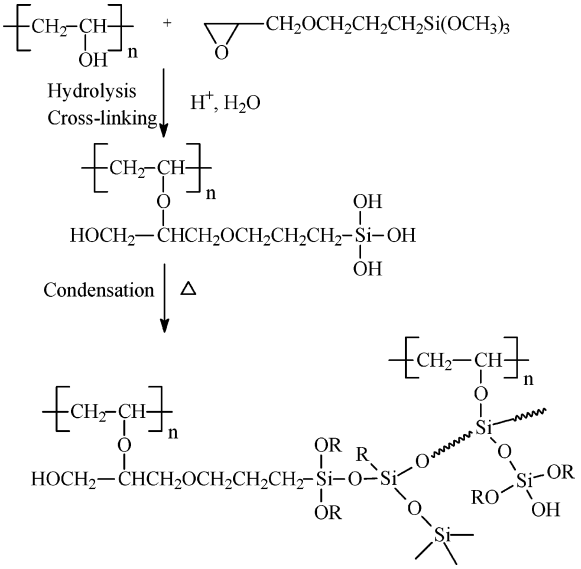

Figure 1. Scheme for the synthesis of PVA-GPTMS hybrid membranes.

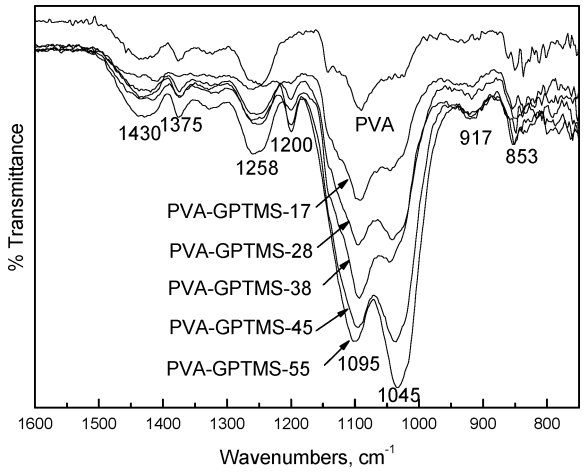

Figure 2. FTIR spectra of the PVA-GPTMS hybrid membranes with different GPTMS content in the 1600−750 cm^{-1} range.

Results and Discussion

Structure of PVA-GPTMS Hybrid Membranes. The possible scheme for synthesis of PVA-GPTMS hybrid membranes is shown in Figure 1. Under acidic conditions, the epoxy ring of GPTMS will open and react with hydroxyl groups of PVA chain to form C−O−C groups. In the process of preparing PVA-GPTMS hybrid membranes, GPTMS is hydrolyzed in the presence of acid catalyst; the resulting silanol group yields siloxane bond due to the dehydration or dealcoholysis reaction with other silanol or methoxyl groups during the membrane annealing. The Si−O−Si linkages formed via the condensation reaction provided interchain covalent bonds and thus resulted in hybrid structure.

The chemical structure of PVA-GPTMS hybrid membranes was analyzed with FTIR and solid-state ^{29}Si-MAS NMR. Figure 2 shows the FTIR spectra in the 1600−750 cm^{-1} range. The band at 917 cm^{-1} is associated with the stretching of Si−OH groups. FTIR results also show the existence of both Si−O−Si groups (1095 cm^{-1})[39] and Si−

(39) Innocenzi, P. *J. Non-Cryst. Solids.* **2003**, *316*, 309.

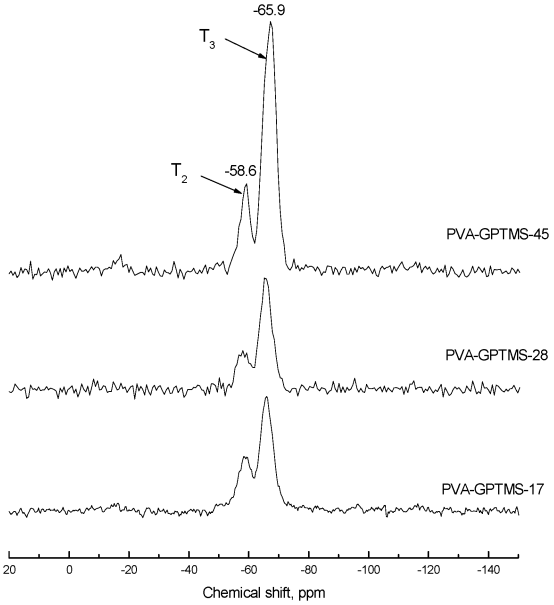

Figure 3. ^{29}Si-MAS NMR of PVA-GPTMS hybrid membrane with different GPTMS content.

O−C groups (1045 cm^{-1}) in the PVA-GPTMS hybrid membranes. It is clear that Si−O−Si groups are the results of condensation reaction between hydrolyzed silanol Si−OH groups. The Si−O−C groups may originate from the condensation reaction between Si−OH groups from hydrolyzed GPTMS and C−OH groups from PVA. The C−OH groups in PVA could react not only with epoxy ring of GPTMS in acid conditions to give C−O−C groups (1200 cm^{-1}) but also with silanol Si−OH groups of GPTMS to give Si−O−C groups. The formation of Si−O−C groups and C−O−C groups will be in favor of better compatibility between organic and inorganic components and a better homogeneity of silica in PVA matrix on the molecular scale.

Figure 3 shows the solid-state ^{29}Si-MAS NMR for PVA-GPTMS hybrid membranes with different GPTMS content. The spectra of PVA-GPTMS hybrid membranes present resonances assigned to T units, which come from the hydrolysis of GPTMS. There are two peaks assigned to T_3-type silicon ($RSi(OSi...)_3$) at −65.9 ppm and T_2-type silicon ($RSi(OSi...)_2(OX)$, X = H, CH_3, or R) at −58.6 ppm.[40] When GPTMS content in hybrid membrane decreases accompanying the weakening of T_3 signal, there is a tendency leading to an overlap between T_2 and T_3 signals in the spectra. The relative ratio of peak intensity of T_2 to T_3 (T_2/T_3) decreases with increasing GPTMS content. T_2/T_3 values are 0.46, 0.35, and 0.26 for PVA-GPTMS-17, PVA-GPTMS-28, and PVA-GPTMS-45 membranes. These changes were quite reasonable considering that hydrogen bonds between PVA and GPTMS exists in the sol−gel process. The strong hydrogen bonding between PVA and GPTMS sols effectively prevented GPTMS sols from complete polycondensation. More GPTMS content in the hybrid membranes leads to more complete polycondensation of GPTMS, and more silica nanoparticle will be thus formed.

(40) Innocenzi, P.; Brusatin, G.; Babonneau, F. *Chem. Mater.* **2000**, *12*, 3726.

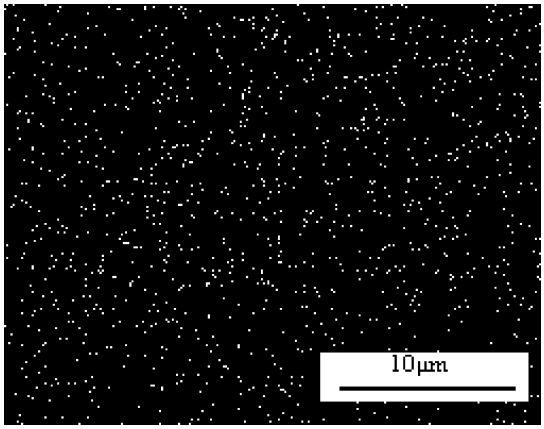

Figure 4. EDX Si-mapping microphotograph of PVA-GPTMS-28 hybrid membrane.

The high transparency of PVA-GPTMS hybrid membranes implied that there should be no macro-phase separation occurring in the hybrid membrane and silica phase homogeneously dispersed in PVA domain. The good compatibility between inorganic component and polymeric component is attributed to the formation of covalent bonding (C−O−C groups and Si−O−C groups) between the two phases. The EDX Si-mapping on the surface of PVA-GPTMS hybrid membranes is shown in Figure 4. It can be found that silica particles (the bright spots) are evenly distributed in the matrix. To confirm this, the morphology is further studied by TEM images. It turns out that the trend of both number and size of formed silica nanoparticles increases with GPTMS content increasing. As shown in Figure 5, silica particles with about 20−50 nm diameter formed when GPTMS content is 28 wt %. The effect of GPTMS content in PVA matrix on hybrid membrane crystallinity is also investigated, which is shown in Figure 6. Due to the semicrystalline character of pure PVA, the pure PVA membrane exhibits a typical peak that appears at $2\theta = 19.6°$. Figure 6 also reveals that pure PVA membrane shows higher crystallinity than those of hybrid membranes. The peak intensity or crystallinity degree of PVA-GPTMS-17 hybrid membrane with lower GPTMS content is less than that of PVA-GPTMS-37 hybrid membranes with higher GPTMS content.

According to the above characterization results, the structure change of PVA-GPTMS hybrid membranes is illustrated in Figure 7. At lower GPTMS content (≤28 wt %), the cross-link structure is formed by the dominant reactions between the PVA and GPTMS and subsidiary reaction between the GPTMS molecules. In this case, a loose chain packing is formed due to the nearly complete destruction of the crystalline region of PVA membrane, and few silica nanoparticles within the membrane can be found. At higher GPTMS content (>28 wt %), the polycondensation reaction between the GPTMS molecules proceeds preferentially and the cross-link reaction between PVA and GPTMS is less favored. Therefore, a rigid chain packing is formed due to the only partial destruction of the crystalline region of PVA membrane, and much more silica nanoparticle within the membrane can be found. The change in the hybrid membrane structure will correspondingly lead to the change of pervaporation properties, which will be discussed later.

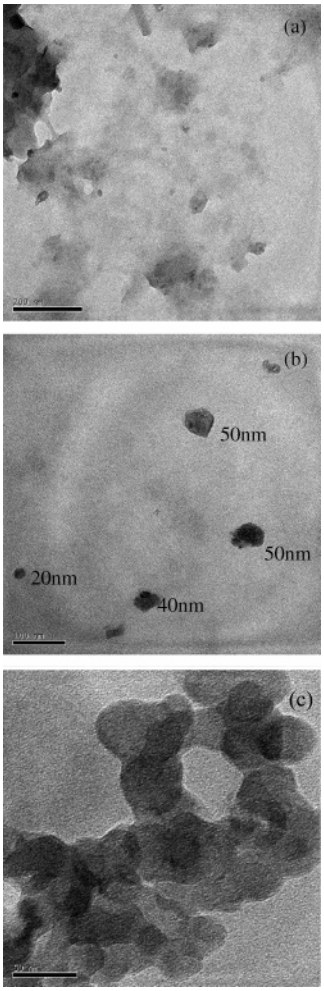

Figure 5. TEM microphotographs of PVA-GPTMS-17 (a) PVA-GPTMS-28 (b) and PVA-GPTMS-45 (c) hybrid membranes.

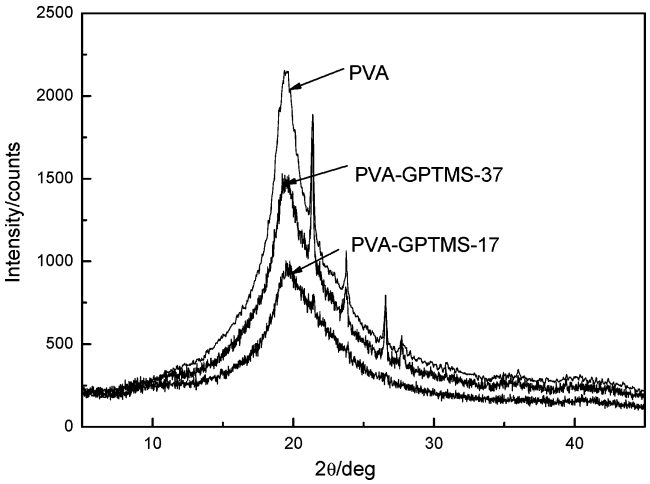

Figure 6. X-ray diffraction patterns of pure PVA membrane, PVA-GPTMS-17, and PVA-GPTMS-37 hybrid membrane.

Thermal Stability and Dynamic Mechanical Behavior. Thermal stability of pure PVA membrane and PVA-GPTMS-28 hybrid membrane was illustrated by TGA curves, which were measured under flowing nitrogen and shown in Figure 8. The hybrid membrane obviously exhibits better thermal stability than that of pure PVA membrane. Moreover, formation of PVA-GPTMS hybrid membrane also increases the char yields (ash amount after TGA analysis) of the

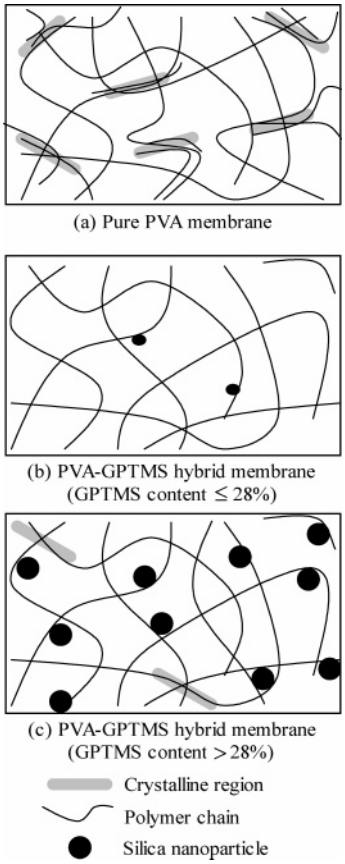

Figure 7. Structure of pure PVA membrane and PVA-GPTMS hybrid membranes with different GPTMS content.

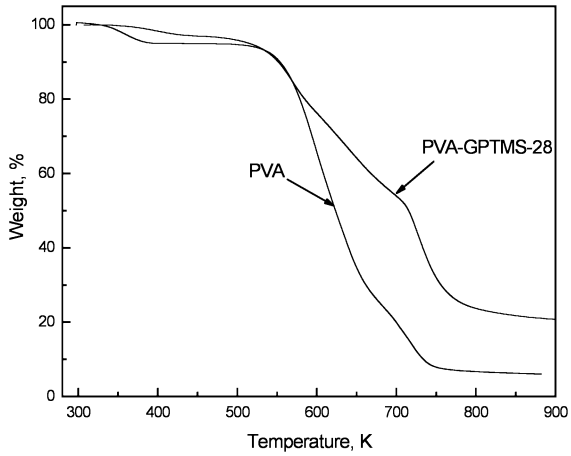

Figure 8. TGA analysis of pure PVA and PVA-GPTMS-28 hybrid membranes.

polymer. Figure 9 shows the dynamic mechanical behavior of pure PVA membrane and PVA-GPTMS-28 hybrid membrane. The Young's modulus of PVA-GPTMS-28 membrane reaches 2.3 GPa at 298 K, which is significantly larger than that of pure PVA membrane (1.2 GPa). As the temperature rises, both pure PVA and PVA-GPTMS-28 membranes exhibit a glass transition region showing a gradually decreasing modulus. The tan δ curves show a peak in the glass transition region. The pure PVA and PVA-GPTMS-28 membrane have a tan δ at 375 and 350 K, respectively. Therefore, it can be seen that T_g of the hybrid membrane is shifted to a considerably lower temperature as compared to that of pure PVA membrane. The decrease of T_g is most

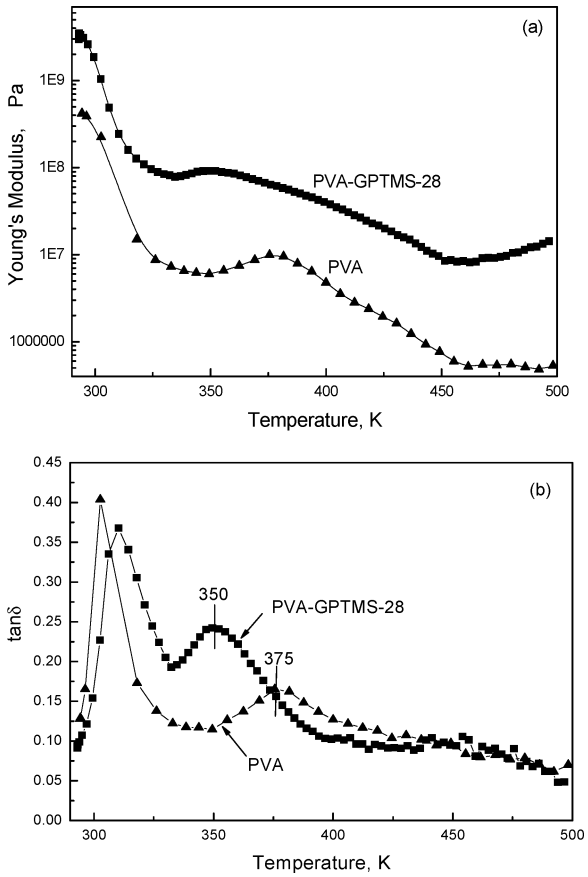

Figure 9. Dynamic mechanical behaviors of pure PVA and PVA-GPTMS-28 hybrid membranes: (a) Young's modulus; (b) tan δ.

possibly caused by hybridization of GPTMS, which decreases the chain stiffness owing to increase of free volume in the hybrid membrane. The ratio of fractional free volume, which is calculated according to PALS experiments, of PVA-GPTMS-28 hybrid membrane to pure PVA membrane is 5.5.[41]

Pervaporation Properties of PVA-GPTMS Hybrid Membranes. The intrinsic tradeoff between permeability and selectivity exists in polymeric membranes. Robenson[2] has summarized the "upper bound tradeoff curve" for O_2/N_2, CO_2/CH_4, etc. gas separation polymeric membranes, which initiates the research of polymeric membrane with high permeability and selectivity. Lue and Peng[3] have collected the pervaporation results on benzene/cyclohexane separation using various membrane materials on 50−60 wt % benzene composition at an operating temperature of 20−80 °C and induced the relationship between benzene/cyclohexane selectivity and benzene flux to plot an upper bound tradeoff

(41) The fractional free volume (FFV) is calculated according to the PALS results. The calculating equation is FFV = $c(V_{F3}I_3 + V_{F4}I_4)$, where V_F is free volume, $V_{Fi} = (4/3)\pi r_i^3$ (i = 3 or 4), I is the intensity of o-Ps, and c is the constant. The r_3 values of pure PVA, PVA-GPTMS-17, PVA-GPTMS-28, PVA-GPTMS-45, and PVA-GPTMS-55 hybrid membranes are 0.22, 0.29, 0.30, 0.26, and 0.25 nm, respectively, and the I_3 values of pure PVA, PVA-GPTMS-17, PVA-GPTMS-28, PVA-GPTMS-45, and PVA-GPTMS-55 hybrid membranes are 4.20%, 8.90%, 10.10%, 9.97%, and 13.47%, respectively. The r_4 values of pure PVA, PVA-GPTMS-17, PVA-GPTMS-28, PVA-GPTMS-45, and PVA-GPTMS-55 hybrid membranes are 0.31, 0.42, 0.41, 0.40, and 0.39 nm, respectively, and the I_4 values of pure PVA, PVA-GPTMS-17, PVA-GPTMS-28, PVA-GPTMS-45, and PVA-GPTMS-55 hybrid membranes are 4.65%, 6.86%, 7.73%, 7.05%, and 5.17%, respectively.

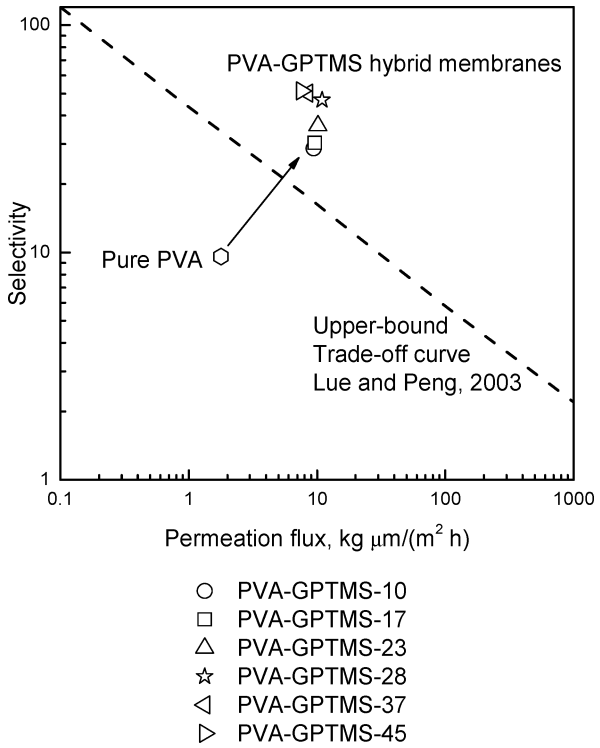

Figure 10. Relationship between the benzene/cyclohexane selectivity and normalized permeation flux of pure PVA and PVA-GPTMS hybrid membranes. Normalized permeation flux (kg μm/(m^2 h) = permeation flux (kg/(m^2 h) $\times$ membrane thickness (μm). Membrane thickness: 80 μm; feed: benzene/cyclohexane (50/50, wt) mixtures; operating temperature: 323 K.

curve shown in Figure 10. According to this upper bound tradeoff curve, in our experiment, the pervaporation properties of pure PVA membrane were obviously below this upper bound tradeoff curve. By hybridization using GPTMS, pervaporation properties of PVA-GPTMS hybrid membranes are all above the upper bound tradeoff curve. The unusual pervaporation properties will be elucidated in the following sections.

Understanding the relationship between polymer structure and membrane performance, in terms of permeability and selectivity, of a polymer membrane enables tailoring of the structure of polymer membrane for specific separation purpose. The permeation of liquid molecules through polymer-based pervaporation membranes occurs via a solution-diffusion mechanism, and the permeability of the penetrant is the product of its solubility and diffusivity. The penetrant diffusivity is dependent on the free volume sizes of the membrane, the size of penetrant molecules, and segmental mobility of polymer chain.

Incorporation of GPTMS with different content into PVA strongly affects membrane properties. As to benzene/cyclohexane (50/50, wt) mixtures at 323 K, permeation flux and separation factor of pure PVA membrane are only 20.3 g/(m^2 h) and 9.6, respectively, while the corresponding values of PVA-GPTMS-28 hybrid membrane are 137.1 g/(m^2 h) and 46.9. To explain the enhancement of permeation flux and separation factor, PALS study was carried out, and the PALS spectra are analyzed using the POSITRONFIT-EXTENDED program (EG&GORTEC). The o-Ps lifetimes and intensities of pure PVA and PVA-GPTMS-28 are shown in Table 1.

Table 1. o-Ps Lifetimes Results Obtained by PALS for Pure PVA and PVA-GPTMS-28 Membranes

sample	τ_3 (ns)	I_3 (%)	r_3 (nm)	τ_4 (ns)	I_4 (%)	r_4 (nm)
PVA	1.35	4.20	0.22	2.29	4.65	0.31
PVA-GPTMS-28	2.15	10.10	0.30	3.68	7.73	0.41

In this study, based on the mechanism of reverse osmosis developed by Matsuura and Sourirajan,[42] it is assumed that there are two types of pores in the polymer-based pervaporation membrane, i.e., network pores and aggregate pores. The network pores are the small cavities between polymer chains constituting the polymer aggregate, whereas the aggregate pores are the large cavities surrounding the polymer aggregates. The PALS results are the first to experimentally show that these pervaporation membranes are composed of two types of pores having radii in the ranges 0.22−0.30 nm from τ_3, network pores, and 0.31−0.41 nm from τ_4, aggregate pores.[41] The radius of a benzene molecule is about 0.263 nm, which is in the range of the network pore size. The radius of a cyclohexane molecule is about 0.303 nm, which is larger than the network pore size. Permeation flux increase of PVA-GPTMS hybrid membranes can be explained by both the size and the number of the two types of pores: (i) Incorporation of GPTMS into PVA membrane enhance the size of both network pores and aggregate pores; therefore, penetrant molecules are easier to permeate through PVA-GPTMS-28 membrane compared with pure PVA membrane. (ii) The number of the two types of pores inevitably increased; that is to say, the permeating pathway of penetrant molecules is increased. Both the size and number of network pores and aggregate pores may contribute to enhancing permeation flux, although the hybrid polymer network forces penetrant molecules to wiggle around the nanoparticles in a random walk, hencing diffusing through a tortuous pathway.

The selectivity of PVA-GPTMS hybrid membranes can be analyzed based on a size-selective mechanism, meaning smaller penetrant molecules (benzene) diffuse faster than larger penetrant molecules (cyclohexane) due to a high fraction of free volume cavities of sufficient size being available for smaller penetrant molecules. The number of network pores of PVA-GPTMS-28 hybrid membrane, which allows only benzene molecules to permeate, increased faster than the number of aggregate pores of PVA-GPTMS-28 hybrid membrane compared with that of pure PVA membrane. Thus, more network pores of PVA-GPTMS hybrid membrane will allow benzene to diffuse easier than cyclohexane. In addition, a tortuous pathway is also favorable for the diffusion of smaller molecules, benzene, over larger molecules, cyclohexane. Therefore, the PVA-GPTMS hybrid membranes show preferential benzene permeability and enhancement of both permeation flux and separation factor.

(42) Matsuura, T.; Sourirajan, S. *Fundamentals of Reverse Osmosis*; NRCC: Ottawa, 1985.

Conclusions

Novel PVA-GPTMS hybrid membranes which successfully solve the tradeoff between permeability and selectivity were prepared by an in situ sol−gel approach. The permeation flux of benzene increased from 20.3 g/(m^2 h) for pure PVA membrane to 137.1 g/(m^2 h) for PVA-GPTMS membrane with 28 wt % GPTMS content, while the separation factor increased from 9.6 to 46.9, simultaneously. The enhanced and unusual pervaporation properties were attributed to the increase in the size and number of both network pores and aggregate pores, and the elongation of the length of the diffusion path in PVA-GPTMS hybrid membranes.

Acknowledgment. We gratefully acknowledge financial support from the Cross-Century Talent Raising Program (Ministry of Education, China), Program for Changjiang Scholars and Innovative Research Team in University (PCSIRT), and SINOPEC Research Program (NO. X503029). We also appreciated the expert help in PALS experiment from Prof. Dashu Yu and Mr. Liqun Wang.

CM051890Q